Compton scattering study of the electronic structure of magnesium hydride

J. Felsteiner, M. Heilper, I. Gertner, A. C. Tanner,* and R. Opher
Department of Physics, Technion—Israel Institute of Technology, Haifa, Israel

K.-F. Berggren
Department of Physics and Measurement Technology, University of Linköping, S-581 83 Linköping, Sweden
(Received 22 September 1980)

Compton scattering measurements have been made on magnesium hydride (MgH_2) using the 59.54-keV gamma rays from a 300-mCi ^{241}Am source at a scattering angle of 150°. Two different theoretical approaches have been used for comparison with the experimental data. In the first approach, the Compton profile of the valence electrons in MgH_2 was calculated by the pseudopotential orthogonalized-plane-wave (OPW) method, including core orthogonalization. In the second approach, the Compton profile of MgH_2 was calculated using the tight-binding linear combination of atomic orbitals (LCAO) method, including large overlaps. Both calculations yielded profiles which are in fairly good agreement with the experimental isotropic profile. The results indicate that the ionic picture of MgH_2 is not simple since its outer electrons are extended. Possible implications of the production process of the hydride are briefly discussed.

I. INTRODUCTION

There is a great interest in metal hydrides as energy storing elements. One of the promising hydrides is MgH_2 which is one of the saline or saltlike hydrides and has a relatively small weight. However, its usefulness is diminished by the slow rate of the reaction $Mg+H_2 \rightleftharpoons MgH_2$. In order to find ways to increase this rate it is obviously of interest to obtain a better understanding of the electronic properties of MgH_2, which quite commonly is referred to as $Mg^{2+}H_2^-$. Such a simplified notation brings to mind the traditional picture of an ordinary ionic crystal with closed-shell ions well localized in space. The properties of MgH_2 appear to be more complex, however, and have therefore, just like LiH, also been discussed in terms of a mixture of ionic, covalent, and metallic bonding.[4] The technique of Compton scattering provides information on the one-dimensional momentum distribution of the electrons.[2] For the purpose of clarifying the true nature of the bonding electrons in MgH_2 we have therefore performed a Compton scattering experiment on polycrystalline MgH_2 using a 59.54-keV ^{241}Am source of 300 mCi.

The notation $Mg^{2+}H_2^-$ immediately suggests that our Compton scattering data are to be interpreted in terms of a simple Heitler-London model with closed-shell ions. Due to the diffuse character of the H^- ions it has been noted, however, that one may choose quite the opposite starting point. Thus a simple "nearly-free-electron" model for MgH_2 has been investigated by Lindner and Berggren.[3] To zeroth order the valence electrons are assumed to form a free gas. Effects of band structure are included in a second-order pseudopotential theory. Their model has the following characteristics: (1) a free-electron gas of valence electrons, (2) a *static* lattice of positive metal ions and bare protons, (3) a pseudopotential form for the electron-metal-ion interaction, and (4) lattice-induced fluctuations in the free gas obtained from pseudopotential theory. The crystal structure of MgH_2 is tetragonal and of the rutile type.[4] There are two Mg^{2+} ions and four protons per elementary cell. The Mg^{2+} ions are at positions $(0,0,0)$ and $(\frac{1}{2},\frac{1}{2},\frac{1}{2})$ and the protons are positioned at $(X,X,0)$, $(1-X,1-X,0)$, $(\frac{1}{2}\pm X,\frac{1}{2}\mp X,\frac{1}{2})$, where $X=0.306$ as can be seen in Fig. 1. In their work, Lindner and Berggren[3] investigated first the stability of the MgH_2 structure. They then calculated the lattice parameters and compared them with the observed ones. For MgH_2 the calculated lattice parameters are $a=4.56$ Å, $c=3.27$ Å, whereas the observed ones are $a=4.52$ Å, $c=3.02$ Å. Thus the calculated lattice parameters and the observed parameters are in fairly good agreement. In the present work we use their nearly-free-electron model in order to calculate the Compton profile of the valence electrons of MgH_2 by means of the pseudopotential orthogona-

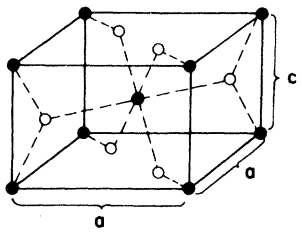

FIG. 1. The unit cell of MgH_2.

lized-plane-wave (OPW) method including core orthogonalization. As a supplement to such a calculation of the MgH_2 Compton profile we have then also investigated the entirely different Heitler-London (or equivalently the tight-binding) approach referred to above; the tight-binding LCAO method, based on Löwdin's symmetrical orthogonalization of atomic orbitals[5] and including large overlaps, was employed. The profiles calculated by both approaches are then compared with experiments. The electronic structure of MgH_2 may have important implications on the production process of this material. In conclusion we therefore briefly speculate about this problem.

II. EXPERIMENTAL PROCEDURE

The experimental arrangement is similar to that described previously[6] and is shown in Fig. 2. The 59.54-keV γ rays were scattered at an angle of $150° \pm 2°$ and detected with a Ge(Li) counter. The 99.9% pure polycrystalline MgH_2 sample[7] was in the form of a disk of 3 mm thickness and 2.6 cm diameter, and about 60 000 counts were accumulated in each channel at the Compton peak. The separation between channels correspond to an interval of approximately 0.06 a.u. per channel.

The raw data were reduced to a Compton profile using the relativistic differential cross section formulas of Ribberfors[8] and transformed into momentum scale q by the relation

$$q = \tfrac{1}{2}(\omega^2 + \omega'^2 - 2\omega\omega'\cos\theta)^{1/2} - \tfrac{1}{2}(\omega - \omega')\left(1 + \frac{2m^2}{\omega\omega'(1-\cos\theta)}\right)^{1/2},$$

where ω, ω' are the incoming and outgoing photon energies and θ is the scattering angle. The data, which were Fourier deconvoluted, still contain a Gaussian resolution function with a full width at half maximum of 0.624 a.u. Approximately 8% of this resolution width results from the angular divergence of the photon beam as calculated by a Monte-Carlo simulation of photon trajectories.

A Monte-Carlo correction for multiple scattering was also included,[9] where the polarization of the photon during its passage through the sample was followed using the formula of Ribberfors for Compton-scattered polarized photons.[10] The final Compton profile (high-energy side) was normalized to an area of 6.6111 from 0 to 6 a.u., according to the area obtained from Hartree-Fock free-atom profiles.[11] The experimental profiles before and after multiple scattering correction are shown in Table I.

III. PSEUDOPOTENTIAL OPW CALCULATION

In this work we use the pseudopotential given by Lindner and Berggren.[3] They described the interaction between Mg^{2+} ions and the valence electrons by a pseudopotential and the interaction between the protons (H^+) and the electrons by a Coulombic potential. Thus we shall write the effective potential V^{ps} as a superposition of the metallic pseudopotential V_M^{ps} and the Coulombic potential of the proton V_P:

$$V^{ps}(\vec{r}) = \sum_{\vec{R}} \left(\sum_{\vec{\sigma}_M} V_M^{ps}(\vec{r} - \vec{R} - \vec{\sigma}_M) + \sum_{\vec{\sigma}_P} V_P(\vec{r} - \vec{R} - \vec{\sigma}_P) \right), \quad (1)$$

where $\vec{R}$ runs over all unit cells, $\vec{\sigma}_M$ and $\vec{\sigma}_P$ run over all the Mg^{2+} ions and the protons in a particular unit cell, respectively, and $\vec{r}$ is the distance from the origin.

The matrix element of the pseudopotential be-

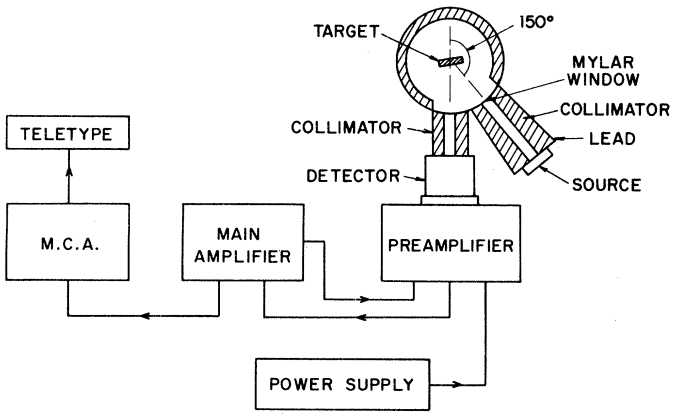

FIG. 2. The experimental arrangement.

TABLE I. Comparison between the experimental Compton profile of polycrystalline MgH_2 and convoluted theoretical profiles.

q (a.u.)	Expt.[a]	Expt.[b]	OPW	LCAO	Free elect.[c]
0.0	4.676	4.737 ± 1.5%	4.785	4.852	5.208
0.1	4.631	4.691	4.746	4.806	5.153
0.2	4.507	4.564	4.630	4.668	4.990
0.3	4.311	4.363	4.400	4.446	4.725
0.4	4.045	4.091	4.184	4.154	4.369
0.5	3.733	3.769	3.875	3.811	3.944
0.6	3.391	3.420	3.527	3.441	3.480
0.7	3.050	3.071	3.163	3.069	3.016
0.8	2.728	2.742	2.805	2.718	2.589
0.9	2.438	2.445	2.473	2.406	2.228
1.0	2.180	2.182 ± 2.5%	2.183	2.140	1.946
1.2	1.778	1.774	1.743	1.745	1.589
1.4	1.513	1.506	1.459	1.483	1.389
1.6	1.317	1.308	1.263	1.291	1.240
1.8	1.152	1.140	1.109	1.133	1.103
2.0	1.016	1.003 ± 3.5%	0.976	0.994	0.975
2.5	0.728	0.713	0.702	0.712	0.702
3.0	0.523	0.511	0.505	0.510	0.505
3.5	0.388	0.379	0.370	0.373	0.370
4.0	0.291	0.284	0.279	0.281	0.279
5.0	0.180	0.178	0.172	0.174	0.172
6.0	0.120	0.120 ± 10%	0.116	0.117	0.116

[a] Experimental (before multiple scattering correction).
[b] Experimental (with multiple scattering correction).
[c] Mg core + 4 free electrons.

tween two plane waves of $\vec{G}_i$ and $\vec{G}_j$ reciprocal lattice vectors is given by

$$V^{ps}(\vec{G}_n)=\frac{1}{\tau}\int e^{-i(\vec{k}+\vec{G}_i)\cdot\vec{r}}V^{ps}(\vec{r})e^{i(\vec{k}+\vec{G}_j)\cdot\vec{r}}d\vec{r}$$

$$=\frac{1}{\Omega}[S_M(\vec{G}_n)V_M^{ps}(\vec{G}_n)+S_P(\vec{G}_n)V_P(\vec{G}_n)]\ , \qquad (2)$$

where $\vec{G}_n=\vec{G}_j-\vec{G}_i$, τ is the crystal volume, and Ω is the unit-cell volume. $V_M^{ps}(\vec{G}_n)$ and $V_p(\vec{G}_n)$ are the Fourier transforms of $V_M^{ps}(\vec{r})$ and $V_p(\vec{r})$, respectively. The "structure factors" in Eq. (2) are defined as

$$S_M(\vec{G}_n)=\sum_{\vec{\sigma}_M}e^{i\vec{G}_n\cdot\vec{\sigma}_M}, \qquad (3)$$

$$S_P(\vec{G}_n)=\sum_{\vec{\sigma}_P}e^{i\vec{G}_n\cdot\vec{\sigma}_P}\ . \qquad (4)$$

Following Ref. 3 we take the following form for the pseudopotential:

$$V_M^{ps}(\vec{G}_n)=-\frac{4\pi Z_M e^2}{G_n^2\epsilon(G_n)}\cos(G_n r_0)e^{-0.03(G_n/2k_F)^4}\ , \qquad (5)$$

where k_F is the Fermi momentum, Z_M is the magnesium atomic number, the parameter r_0 is equal to 1.390 a.u., and $\epsilon(G_n)$ is the dielectric function of an insulator as given in Ref. (12). $V_P(\vec{G}_n)$ is simply the screened Coulombic potential:

$$V(\vec{G}_n)=-\frac{4\pi e^2}{G_n^2\epsilon(G_n)}\ . \qquad (6)$$

In the OPW method one writes the wave function $|\psi\rangle$ of a valence electron as

$$|\psi\rangle=|\phi\rangle-\sum_c\langle\psi_c|\phi\rangle|\psi_c\rangle\ , \qquad (7)$$

where $|\phi\rangle$ is the pseudo wave function and $|\psi_c\rangle$ is a core electron wave function. The pseudopotential equation is given by

$$\left(\frac{p^2}{2m}+V^{ps}(\vec{r})\right)|\phi\rangle=E|\phi\rangle\ . \qquad (8)$$

From solving Eq. (8) one obtains the true energy eigenvalues and the pseudo wave function $|\phi\rangle$. The order of the matrix that we used for diagonalization was 207×207 and the convergence for the eigenvalues (which are the energy bands) was satisfactory (the difference between two different orders of matrices was 0.004 Ry).

It can easily be shown that the momentum density $\rho(\vec{p})$ of the valence electrons is given by

$$\rho(\vec{p})=2|A_{\vec{G}_n}(\vec{p}-\vec{G}_n)|^2[1-|f(\vec{p})|^2]^2\ , \qquad (9)$$

where $A_{\vec{G}_n}$ is defined by

$$\phi(\vec{k},\vec{r})=\frac{1}{\sqrt{\tau}}\sum_{\vec{G}_n}A_{\vec{G}_n}(\vec{k})e^{i(\vec{k}+\vec{G}_n)\cdot\vec{r}} \qquad (10)$$

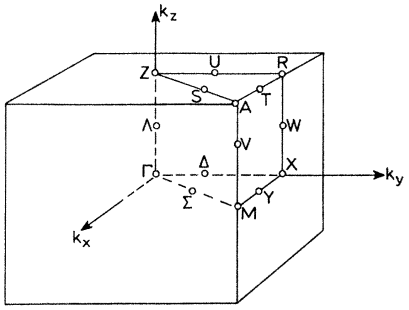

FIG. 3. The first Brillouin zone of MgH_2.

and $\vec{p}=\vec{k}+\vec{G}_n$. $f(\vec{p})$ is the core orthogonalization contribution and is given by

$$f(\vec{p})=\frac{1}{\Omega}\sum_c \frac{|\int a_c(\vec{r})e^{-i(\vec{k}+\vec{G}_n)\cdot\vec{r}}d\vec{r}\,|^2}{\Sigma_R e^{i\vec{k}\cdot\vec{R}}S_{cc}(\vec{R})} \tag{11}$$

The summation on c is on all core orbitals, $a_c(\vec{r})$ is an atomic orbital, and

$$S_{cc}(\vec{R})=\int a_c^*(\vec{r})a_c(\vec{r}+\vec{R})d\vec{r} \tag{12}$$

is an overlap integral. The atomic orbitals a_c were taken from Ref. 13.

In order to get the isotropic Compton profile, we have to average $\rho(\vec{p})$ over all possible directions. We performed an approximate spherical average according to

$$\langle\rho(\vec{p})\rangle=\tfrac{1}{26}(4\rho_{100}+4\rho_{110}+2\rho_{001}+8\rho_{011}+8\rho_{111}), \tag{13}$$

where 100, 110, 001, 011, and 111 are, respectively, the directions Γ-A, Γ-R, Γ-Z, Γ-M, Γ-X, in the first Brillouin zone (see Fig. 3). Using this averaging, we obtain the isotropic Compton profile

$$J(q)=2\pi\int_{|q|}^{\infty}\langle\rho(\vec{p})\rangle p\,dp\,, \tag{14}$$

where $\langle\rho(\vec{p})\rangle$ is given by Eq. (13).

As we can see in Eq. (9), the term which describes the wiggling part of the wave function is $[1-|f(\vec{p})|^2]^2$ [when $f(\vec{p})=0$ we obtain the momentum density in the smooth wave-function approximation]. Since the Fourier transform of a localized function is smeared, one may generally assume that the contribution of the wiggling part of the wave function at the peak region of the Compton profile is small. In order to check this assumption we calculated this contribution explicitly and it turned out to be less than 0.1% at the peak of the profile. The total Compton profile which is the sum of the OPW valence profile and the core profile[11] is given in Table II.

TABLE II. Theoretical Compton profiles of polycrystalline MgH_2.

q (a.u.)	OPW	LCAO	Free elect.[a]	Mg core
0.0	5.082	5.166	5.604	1.990
0.1	5.027	5.163	5.541	1.980
0.2	4.899	5.006	5.364	1.960
0.3	4.698	4.738	5.088	1.948
0.4	4.406	4.385	4.696	1.924
0.5	4.064	3.942	4.201	1.902
0.6	3.628	3.433	3.587	1.867
0.7	3.141	2.925	2.856	1.820
0.8	2.652	2.492	2.012	1.765
0.9	2.220	2.165	1.716	1.716
1.0	1.928	1.933	1.658	1.658
1.2	1.616	1.640	1.519	1.519
1.4	1.406	1.440	1.384	1.384
1.6	1.233	1.271	1.231	1.231
1.8	1.099	1.119	1.099	1.099
2.0	0.965	0.981	0.965	0.965
2.5	0.691	0.700	0.691	0.691
3.0	0.496	0.501	0.496	0.497
3.5	0.363	0.367	0.363	0.363
4.0	0.274	0.277	0.274	0.275
5.0	0.171	0.172	0.171	0.171
6.0	0.116	0.117	0.116	0.116

[a] Mg core + 4 free electrons.

IV. TIGHT-BINDING LCAO CALCULATION

The LCAO approach is expected to give good results in ionic crystals where tight binding and localization of the electrons around the crystal ions is the real picture. As we shall see, the Compton profile calculated in this way agrees quite well with the experimental profile provided we include large overlaps. We used wave functions Mg^{2+} from Ref. 13, and H^- wave functions from Ref. 14.

The general expression $J_{\hat{k}}(q)$ is[15]

$$J_{\hat{k}}(q)=\sum_{\alpha=1}^{r}\sum_{t=0}^{\infty}n_t^{\alpha}\sum_{n',l'\in g_t^{\alpha}}\sum_{n,l\in g_0^{\alpha}}(\Delta^{-1})_{\alpha 0nlm_1,\alpha tn'l'm_1}\sum_{\lambda=|l-l'|}^{l+l'}\beta_{\lambda}(l\,m_1;l'-m_1)\int_{|q|}^{\infty}g_{\hat{k},\lambda t}^{\alpha}(p,q,R_t^{\alpha})P_{nl}^{\alpha 0}(p)P_{n'l'}^{\alpha t}(p)p\,dp\,, \tag{15}$$

where $\hat{k}$ is a unit vector in the direction of the scattering vector and the z axis of the coordinate system was chosen parallel to $\hat{k}$. q is the electron momentum projection on z axis, r is the number of basis atoms in the unit cell, n_t^{α} is the number of atoms q_t^{α} which are neighbors of order t of g_0^{α}—the αth atom in the unit cell. Each atom has several orbitals denoted by n, l, m, and n', l', m', respectively. Selection rules preclude the possibility of $m\neq m'$. The term $(\Delta^{-1})_{\alpha 0nlm_1,\alpha tn'l'm_1}$ is the appropriate term of the inverse overlap matrix Δ whose elements are the overlap integrals between the electronic wave function

with quantum numbers n, l, m_1 centered on g_0^α, and the wave function with quantum numbers n', l', m_1 centered on g_t^α at a distance $\vec{R}_{ts}^{\alpha}$; this is the position of the sth neighbor of order t with respect to g_0^α:

$$\beta_\lambda(lm;l'm') = (-1)^{(2m'-l+l'+\lambda)/2}[(2l+1)(2l'+1)]^{1/2} C(ll'mm'|\lambda m+m')C(ll'00|\lambda 0)\,, \tag{16}$$

where the C's are the Clebsch-Gordan coefficients.

$$g_{\vec{k},\lambda t}^{\alpha}(p,q,R_t^\alpha) = 2(-i)^\lambda(2\lambda+1)^{-1}\sum_m (n_t^\alpha)^{-1}\sum_{s=1}^{n_t^\alpha} Y_\lambda^m(\Omega_{\alpha 0,\,\alpha ts})^* \int_0^{2\pi} Y_\lambda^m(\Omega)\exp(i\vec{p}\cdot\vec{R}_{ts}^{\alpha})d\phi\,|_{\cos\theta=q/p}\,, \tag{17}$$

$P_{nl}^{\alpha 0}(p)$ and $P_{n'l'}^{\alpha t}(p)$ are the radial parts of the Fourier transforms of the given orbitals.

The expression (15) is much simplified after averaging over all directions of the scattering vector $\hat{k}$ as needed in isotropic Compton profile calculation. This brings $g_{\langle\hat{k}\rangle,\lambda t}^{\alpha}(p,q,R_t^\alpha)$ to the final form $j_\lambda(pR_t^\alpha)$ which is the spherical Bessel function of order λ of the argument pR_t^α. Further simplification of $J_{\langle k\rangle}(q)$ is achieved by assuming that each ion contributes only one occupied s state whose overlap integral with any electron orbital on a neighboring ion is non-negligible. For the H^- orbital this assumption is fulfilled automatically because there is only the occupied $1s$ orbital. Calculating all the overlap integrals with the Mg^{2+} ion, we have found that in addition to the contribution from the $H^-(1s)-H^-(1s)$ overlap, the only other non-negligible contribution is from the $Mg^{2+}(2s)-H^-(1s)$ overlap; all other overlap terms are much smaller and can be neglected. Such a conclusion was also drawn by Aikala[16] in the case of Ca where terms except the $4s$ were neglected in the overlap calculations. We followed the procedure given by Aikala[15] and found the expression for the isotropic Compton profile to be

$$J_{\langle\hat{k}\rangle}(q) = \sum_{\alpha=1}^{\kappa}\sum_{t=0}^{\infty} n_t^\alpha \sum_{n',l'}^{g_t^\alpha}\sum_{n,l}^{g_0^\alpha}(\Delta^{-1})_{\alpha 0_n\, lm_1,\,\alpha t_{n'}\, l'm_1}\int_{|q|}^{\infty} j_0(pR_t^\alpha)P_{nl}^{\alpha 0}(p)P_{n'l'}^{\alpha t}(p)p\,dp\,. \tag{18}$$

The calculations used the analytic form of the wave functions,[13,14] and due to the inclusion of the overlap of s orbitals only, we could use a simple subroutine for matrix inversion appropriate to a symmetric positive matrix only. While increasing t in Eq. (18), which is equivalent to including more and more neighbors in the calculation, we checked the convergence of $J_{\langle\hat{k}\rangle}(q)$ and found the inclusion of 162H^- and Mg^{2+} ions to be satisfactory. The Compton profile which resulted from this LCAO calculation is given in Table II.

V. DISCUSSION

Table II shows the calculated Compton profiles of polycrystalline MgH_2 for both the OPW and the LCAO methods along with the profile constructed from an Mg core[11] and that of four free electrons using the formula

$$J_{\text{free}}(q) = \frac{3N_e}{4p_F}\left[1-\left(\frac{q}{p_F}\right)^2\right],$$

where $N_e=4$ and $p_F=0.829$ a.u. Since the final experimental profile still contains a Gaussian resolution function of FWHM = 0.624 a.u., the calculated profiles have been convoluted with this resolution width and are then compared with the experimental profile in Table I.

It is seen that the OPW profile agrees well with the experimental profile, which immediately implies that the valence electrons in MgH_2 are not localized as in an ordinary ionic crystal. One may say that the reason that MgH_2 is an insulator (or it may also be referred to as a semiconductor) is due to the fact that its valence band is filled and its conduction band empty. At the same time we note that the LCAO profile, although it is a bit higher at the peak than the OPW profile, also agrees fairly well with both experiment and with the OPW calculation. This is in spite of the fact that we here used quite an opposite starting point. Then the question to be asked is whether the four valence electrons in MgH_2 indeed are more or less "free" and their distribution resembles that of a nearly-free-electron gas, as implied by the nice agreement between measured values and the OPW profile, or whether the contrary is true. At a first glance one may in fact conclude from the almost equally satisfactory agreement between the tight-binding LCAO isotropic Compton profile and experiment that an ionic picture with well localized charges is equally true. In principle there is the possibility that the Compton scattering technique would be too insensitive to distinguish between the two configurations. This perhaps puzzling situation may be clarified if we check some of the properties of the H^- ion in MgH_2. The free hydrogen wave function is very diffuse. The

classical ionic crystal radius of H^- is, according to Pauling,[17] 2.08 Å which is to be compared with the $H^- - Mg^{2+}$ distance of 1.95 and 2.48 Å between H^- and H^- in the MgH_2 crystal. This comparison indicates that the H^- free ion wave function when placed in the crystal environment will penetrate appreciably into regions beyond the nearest neighbors and will be very much deformed. The large overlap between H^- ions and the associated diffuse or delocalized character of the charge clouds then require that a large number of neighbors is taken into account. Convergence of the LCAO profile is only achieved if the overlaps of 162 ions are considered. For example, the inclusion of only 37 ions neither gives results that are in agreement with experiment nor even a correct physical shape of the computed Compton profile. The inclusion of a large number of neighbors in the calculation results in quite a smooth charge distribution of the outer electrons as in a nearly-free-electron gas. Thus the oversimplified ionic picture, which was our initial motivation, and the nearly-free-electron model led us to the same conclusion. The large overlaps, of course, explain why the nearly-free-electron model or a plane-wave expansion works so well. It may be a matter of taste which approach is to be preferred. In our opinion, however, the nearly-free-electron model is so much easier to implement. We therefore suggest that it should be used in any calculation dealing with the charge and momentum distribution in MgH_2.

The nature of the valence electrons in MgH_2 may have important implications on the production process of this material. The process is as follows. First, hydrogen gas is pressurized onto the surface of the magnesium metal and an initial thin layer of MgH_2 is formed.[18] Then in order to let more hydrogen combine with magnesium, either hydrogen would have to diffuse through the initial MgH_2 layer and combine with Mg at the interface between this layer and the metal, or, alternatively, the magnesium ions would have to diffuse through the initial MgH_2 layer and combine with the hydrogen at the interface between this layer and the gas. Such a diffusion through the hydride is known to be the most important rate-controlling transport process. It is also known that the diffusion equations do not distinguish between hydrogen and magnesium; either of them can diffuse.

Mintz *et al.*,[19] taking into account that the classical radius of the H^- ion (~2.08 Å) is much larger than that of Mg^{2+} (~0.65 Å), assumed that the Mg^{2+} ions diffuse and not the H^- ions. Also Stander[20] has recently presented model calculations from which he has concluded that Mg^{2+} rather than H^- is the diffusing species in MgH_2. Mintz *et al.* therefore suggested that the Mg^{2+} diffusion rate could be improved by doping, for example, Ga^{3+} ions into the hydride, thereby producing vacancies at Mg^{2+} sites. Luz *et al.*,[18] on the other hand, describe a model in which the hydrogen diffuses through the hydride layer and not magnesium. In fact they were able to photograph the sample and to see that indeed there is some growing from the hydride layer into the metal.

Our conclusion above about the valence electrons in MgH_2 is that they are not appreciably localized in space. From this one may expect that in the hydride we do not have rigid H^- ions with a large ionic radius, as argued by Mintz *et al.*,[19] but just protons that can diffuse much more easily through the hydride lattice. This picture is not entirely correct either. The nearly-free-electron model rather leads us to describe the diffusing species as a proton accompanied by a polarization cloud of electrons. The effective charge of such an entity is, let us say, $-\delta$, where $\delta < 1$. In the same way the Mg ions carry an electron cloud such that the effective charge is $+2\delta$. In this way one may retain an ionic description for transport and diffusion processes and effectively write $Mg^{+2\delta}H_2^{-\delta}$. With this description, a proton dressed by a polarization cloud, it appears that the diffusion of $H^{-\delta}$ could take place more easily than the rigid H^- ion assumed by Mintz *et al.*[19] At the same time there is no argument why diffusion of $H^{-\delta}$ should be more favored than $Mg^{+2\delta}$. Instead we suggest that the diffusion of $H^{-\delta}$ takes place via vacancies occurring in the following way. At the interface between the metal and the hydride the screening changes character and becomes metallic. As a consequence a proton at this interface behaves more like a proton in a metal, i.e., the proton and its polarization cloud becomes a neutral entity. As such it can more easily diffuse into the Mg metal where it is almost completely screened off from the hydride by the metallic electrons. The remaining vacancy now opens a diffusion channel for hydrogen. Such a mechanism would favor the work of Luz *et al.*[18] It also suggests that in order to improve the production process of MgH_2 efforts should be made to find ways to improve the diffusion rate of protons into the magnesium metal and hydrogen through MgH_2, rather than the diffusion of the Mg^{2+} ions.

Note added in proof. Recently G. L. Krasko has investigated the electronic structure of MgH_2 (unpublished). The basic approach is similar to ours, i.e., a plane wave expansion and pseudopotential theory. Perturbation techniques are,

however, used instead of our diagonalization procedure. Krasko finds, as we do, that the bonding in MgH_2 cannot be considered as purely ionic.

ACKNOWLEDGMENTS

This work was supported in part by a grant from the National Council for Research and Development, Israel, and the KFA Jülich, Germany.

---

*Present address: Chemistry Department, Florida State University, Tallahassee, Florida 32306.

[1]G. G. Libowitz, *The Solid State Chemistry of Binary Metal Hydrides* (Benjamin, New York, 1965).
[2]*Compton Scattering*, edited by B. Williams (McGraw-Hill, London, 1977).
[3]P. Lindner and K.-F. Berggren, Int. J. Quantum Chem. 7, 667 (1973).
[4]*Metal Hydrides*, edited by W. H. Mueller, J. P. Blackledge, and G. G. Kobowitz (Academic, New York, 1968).
[5]P. O. Löwdin, Adv. Phys. 5, 1 (1956).
[6]P. Pattison, S. Manninen, J. Felsteiner, and M. Cooper, Philos, Mag. 30, 973 (1974); S. Manninen, T. Paakkari, and K. Kajantie, Philos. Mag. 29, 167 (1974).
[7]Prepared by P. S. Rudman and J. Genossar, Technion, Haifa.
[8]R. Ribberfors, Phys. Rev. B 12, 2067 (1975).
[9]J. Felsteiner, P. Pattison, and M. Cooper, Philos. Mag. 30, 537 (1974); J. Felsteiner and P. Pattison, Phys. Rev. B 13, 2702 (1976).
[10]R. Ribberfors, Phys. Rev. B 12, 3136 (1975).
[11]F. Biggs, L. B. Mendelsohn, and J. B. Mann, At. Data Nucl. Data Tables 16, 201 (1975).
[12]J. L. Fry, Phys. Rev. 179, 892 (1969).
[13]E. Clementi and C. Ruetti, At. Data Nucl. Data Tables 14, 177 (1974).
[14]L. D. Landau and E. M. Lifshitz, *Quantum Mechanics* (Pergamon, New York, 1965), p. 240.
[15]O. Aikala, Doctoral thesis, University of Turku, 1977, p. 32.
[16]O. Aikala, Philos. Mag. 31, 935 (1975).
[17]L. Pauling, *The Nature of the Chemical Bond* (Cornell University Press, Ithaca, New York, 1945).
[18]Z. Luz, J. Genossar, and P. S. Rudman, J. Less-Common Met. (unpublished).
[19]M. H. Mintz, S. Malkiely, Z. Gavra, and Z. Hadari, J. Inorg. Nucl. Chem. 40, 1949 (1978).
[20]C. M. Stander, S. Afr. J. Chem. 32, 79 (1979).